Supplemental Data

Virus Capsid Expansion Driven

by the Capture of Mobile Surface Loops

Kelly K. Lee, Lu Gan, Hiro Tsuruta, Crystal Moyer, James F. Conway, Robert L. Duda, Roger W. Hendrix, Alasdair C. Steven, and John E. Johnson

Supplemental Experimental Procedures

Construction of the ΔEloop Mutant

For the first round PCR, plasmid DNA was diluted 100-fold; extracted gel bands were used undiluted for the second round. First round thermo-cycling was performed at 94 ˚C for 30 s, 50 ˚C for 30 seconds and 72 ˚C for 2.5 min for 15 cycles. The second round PCR used initial cycles at a higher annealing temperature: 94 ˚C for 30 sec, 65 ˚C for 30 seconds and 72 ˚C for 2.5 min for 5 cycles, followed by 10 cycles as given above. The initial template was plasmid pV0-SacI, a variant of HK97 expression plasmid pV0 (pT7-5Hd2.9 in (Duda et al., 1995)) in which the 3rd codon GAA of gp5 is replaced with GAG to create a unique SacI site. The two first round PCR reactions used primers CGGAAACGAAGCACAAATAAA (upstr2for) together with ATCCGAATCGCCCGGCGCATTGGTAAACACCTCTTC (E-APGD-rev), and TCAATCTGCTGCTTAAACAGA (downst2rev) together with ACCAATGCGCCGGGCGATTCGGATATCACCTTCAGC (E-APGD-for). The two PCR products with overlapping ends produced in the first round were gel purified, mixed and amplified in the second round using only outer primers upstr2for and downst2rev. The product was purified using a Qiagen kit, cut with restriction enzymes *SacI* and *KpnI*, and the resulting 648 bp fragment was used to replace the 675 bp *SacI-KpnI* fragment in plasmid pV0-SacI by ligation to the large fragment from a *SacI-KpnI* digest of the plasmid.

Conversion of P-II to EI-I is Independent of Crosslinking

We demonstrated previously that the WT HK97 Prohead-II capsid reorganizes into EI-I in a highly cooperative, two-state manner (Lee et al., 2005). No stable, long-lived particle form intermediate in size between P-II and EI-I was observed to exist. Complete conversion of a population of P-II particles takes approximately 5 min in pH 3.9, 500mM KCl, and occurs prior to the formation of substantial numbers of crosslinks. To confirm that this earliest stage of the maturation pathway is crosslink-independent, we used time-resolved SAXS to examine the acid-induced maturation of 3 crosslink-deficient HK97 variants, including trypsinized WT (trpWT) P-II and two mutants, ΔEloop and K169Y. Trypsinization of WT P-II cleaves at a single site, after Lys-166 on the E-loop (Duda et al., 1995). The ΔEloop mutant has a truncated E-loop with 13 residues (residues 159-171, which includes the crosslinking residue Lys-169) replaced by an abbreviated reverse turn (sequence Ala-Pro-Gly-Asp). The K169Y mutant is a residue substitution that, likewise, renders the particles crosslink-deficient.

The acid stage of maturation for WT, trpWT, K169Y, and ΔEloop P-II particles was induced by diluting a concentrated stock of P-II particles into 250mM KCl, pH 3.9 buffer with a final particle concentration of approximately 5 mg/ml. A series of 55 3s SAXS exposures were gathered at 60s (first 30 exposures) and 120 s (last 25 exposures) intervals. As shown in Supplementary Figure 1, trpWT particles undergo the acidification stage of maturation in a similar fashion and at similar rate to native WT particles. The transition is a two-state process as determined by the clear presence of isoscattering points throughout the angular range and by singular value decomposition (SVD) analysis (see reference (Lee et al., 2005)). K169Y P-II particles undergo the transition at a similar rate to WT and trpWT (Supplementary Figure 1). The P-II to EI-I conversion for this

mutant is also two-state. Likewise, the ΔEloop mutant behaves similarly to trpWT and native WT particles (not shown). These results confirm that the early stage of HK97 capsid maturation is crosslink-independent.

***Ab initio* Shape Reconstruction of EI-II Particles Based Upon SAXS Measurements**

Two separate SAXS patterns covering low (Q=0.005-0.15; d=1250-40 Å) and high (Q=0.04-0.5; d=150-12 Å) angle ranges were measured for P-II and EI-II particles. These were merged by standard procedures and then analyzed using GNOM to obtain the P(r) pairwise electron distributions (Svergun, 1991). Maximal dimensions (D_{max}) of 565 Å for EI-II and 540 Å for P-II, and radii of gyration of 263 Å for EI-II and 232 Å for P-II were determined. GNOM results were then input into a reconstruction process developed by Svergun *et al* and implemented in the program DAMMIN v5.1 (Svergun, 1999). DAMMIN constructs a scattering model from a lattice of scattering beads and iteratively optimizes the bead positions to produce the best match to the measured SAXS pattern (P(r) electron distribution function). Icosahedral (5-fold, 3-fold, 2-fold) symmetry was imposed in the reconstruction process. With the exception of smaller dummy atom sizes, 12-14 Å, default settings were applied in DAMMIN. The program CRYSOL was used to compute the SAXS pattern from the EI-I/II pseudoatomic model (Svergun, 1995). As Supplementary Figure 2 shows, very good agreement between SAXS-determined structure and the cryo-EM-based pseudoatomic model for EI-I/II was found, confirming that the particles that exhibit the ladder crosslink pattern in our experiments were in the EI-I/II particle state.

Supplemental References

Duda, R.L., Hempel, J., Michel, H., Shabanowitz, J., Hunt, D., and Hendrix, R.W. (1995). Structural transitions during bacteriophage HK97 head assembly. J Mol Biol *247*, 618-635.

Lee, K.K., Tsuruta, H., Hendrix, R.W., Duda, R.L., and Johnson, J.E. (2005). Cooperative reorganization of a 420 subunit virus capsid. J Mol Biol *352*, 723-735.

Svergun, D.I. (1991). Mathematical Methods in Small-Angle Scattering Data Analysis. J Appl Cryst *24*, 485-492.

Svergun, D.I. (1995). CRYSOL- a Program to Evaluate X-ray Solution Scattering of Biological Macromolecules from Atomic Coordinates. J Appl Cryst *28*, 768-773.

Svergun, D.I. (1999). Restoring low resolution structure of biological macromolecules from solution scattering using simulated annealing. Biophys J *76*, 2879-2886.

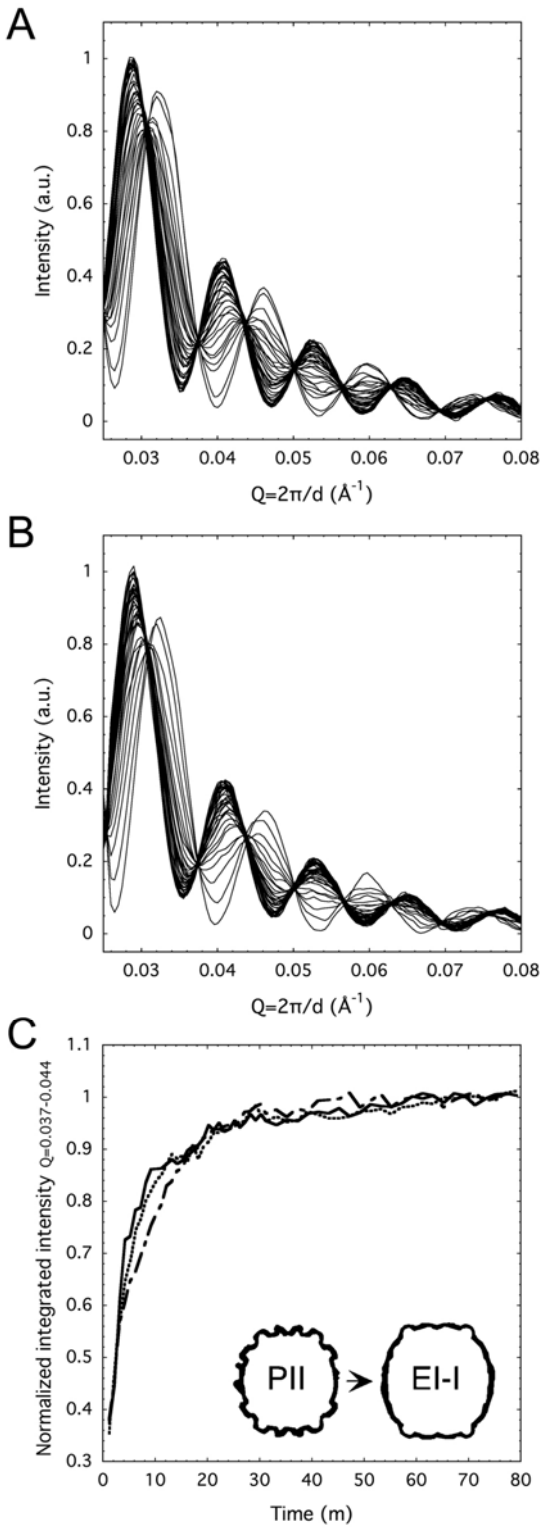

Figure S1. The First Stage of HK97 Capsid Maturation, In Which P-II Converts to the EI-I Particle Form Is Not Dependent on Crosslink Formation

This is demonstrated by the similarity in time-resolved SAXS observed for P-II acid-induced maturation with wild type (not shown; see Lee et al., 2005), crosslink-defective, trypsinized WT (trpWT) (A), and crosslink-defective K169Y (B) particles. We have demonstrated previously that, for wild type particles, this transition occurs in a cooperative, two-state fashion (Lee et al., 2005). The kinetics of the P-II to EI-I transition are essentially identical for crosslink-capable and crosslink-defective variants of the particles (C); WT kinetics shown with solid line, trpWT with dotted line, and K169Y with dash-dotted line.

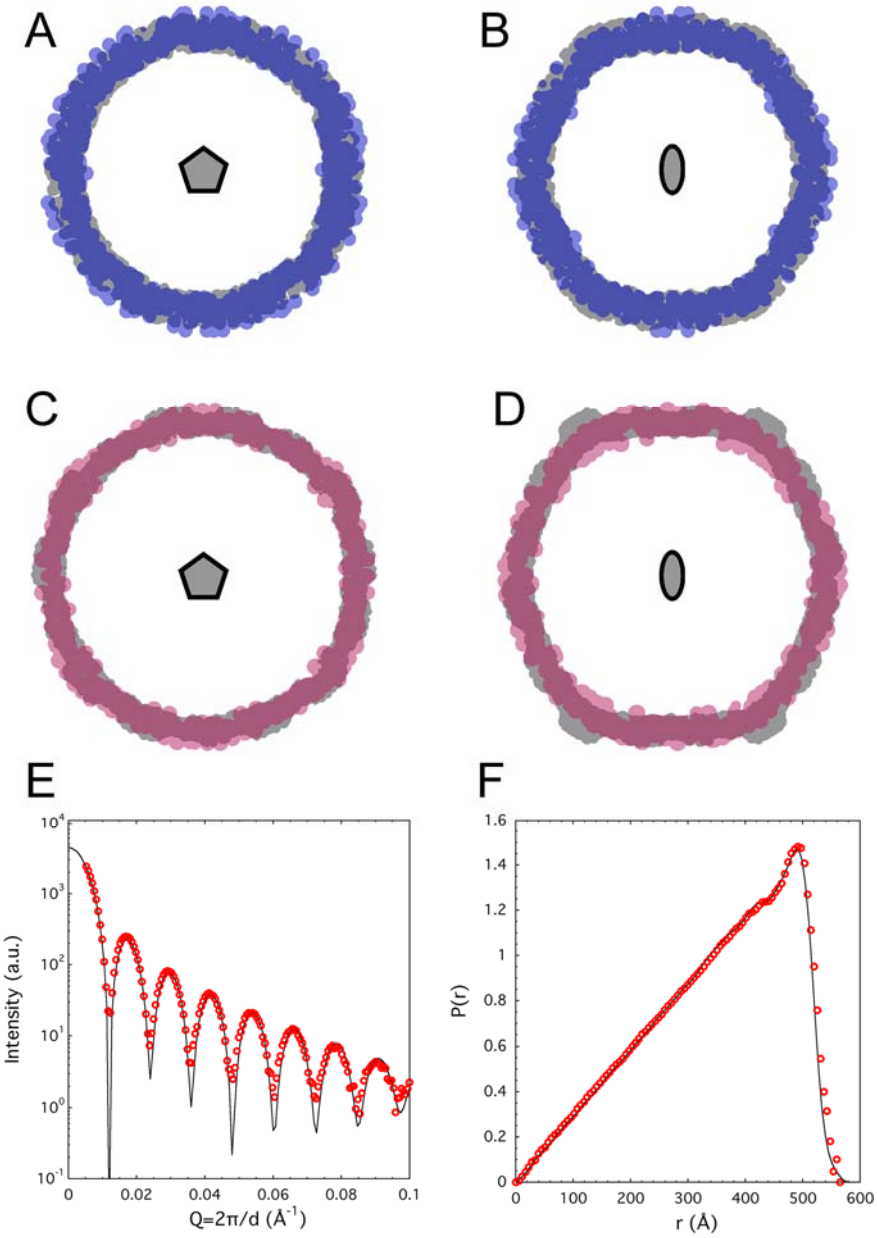

Figure S2. Consistency of Particle Morphologies Measured by SAXS and by Cryo-EM

(A) A cross-sectional view down the 5-fold icosahedral axes of an *ab initio* SAXS-based reconstruction of P-II particles (blue), superimposed upon the cryo-EM and crystallography-based pseudoatomic model for P-II (grey; Conway et al., 2001). The overall shape and size of the two models are in excellent agreement. The *ab initio* reconstruction algorithm also captures the essential features of shell thickness.
(B–F) Similar comparison viewed down the 2-fold axes. When similar procedures are applied to measured SAXS data for the EI-II particles, which exhibit ladder crosslink patterns, good agreement between the *ab initio* reconstructed SAXS model (red) and the pseudoatomic model derived from cryo-EM and rigid body fitting of high resolution subunit structures into the EM density (grey) is observed (C and D). Excellent agreement is observed between the SAXS pattern that we calculate from the EI-I/II pseudoatomic model, and measured SAXS data for the EI-II particles (E). The pair-wise electron distribution plot (spherically averaged Patterson plot) shown in (F) confirms that the SAXS-based and cryo-EM based models are consistent.